Dynamic calculation of nonlinear magnetic circuit for computer aided design of a fluxgate direct current sensor

Takafumi Koseki(The Univ. of Tokyo) , Hiroshi Obata(The Univ. of Tokyo) ,
Yasuhiro Takada(The Univ. of Tokyo), Cheung Cheuk Kei Brian (The Univ. of Tokyo) ,
Eric Favre(LEM-SA), Toshifumi Tachibana, Yori Hatakeyama(LEM-Japan)

The University of Tokyo
Engineering Building#2 12F, 7-3-1 Hongo
Bunkyo-ku, Tokyo 113-8656, Japan

Abstract

The research proposes how to cancel AC noise when fluxgate direct current sensor has AC noise. The authors propose an active AC cancellation and evaluate compensation effects by simulation and experiment. Both simulation and experiment results are shown the 2*nd* harmonic level disturbance effects are the largest. The authors confirmed the active cancellation method for the disturbances. This paper explains the background of fluxgate sensor in the chapter. In the second chapter the author explain the principle and structure of the sensor. In the third chapter simulation results with P-spice and Matlab are shown and in the fourth chapter experimental results are shown. In the last chapter the authors refer to the conclusion of this research.

Keywords: Fluxgate sensor, AC noise, Active AC compensation, Dynamic response calculation.

1 INTRODUCTION

Current sensors are used widely in the control and observation of countless electronic products, testing for the stability of current flows and loss in the system. Among them, the fluxgate current sensor is a highly sensitive current sensor for the testing of DC and is used at room temperatures. Its simplicity and durability in design gives it high commercial values. A single-core fluxgate current sensor consists fundamentally of a soft magnetic core, a coil for generating high amplitude magnetic signal as well as to test for the change in magnetic flux density.

In general, the fluxgate technology offers the following advantages. Firstly, low offset and offset drift, because the magnetic core is cycled through its hysteresis loop, suppressing any magnetic offset in the fluxgate core. Secondly, excellent accuracy due to quasi absence of offset resulting in higher speed in response time. Compared to Hall based technologies, this advantage is more noticeable for small current measurement, where the relative effect of the offset is more significant. Thirdly, a large dynamic range allowing measurement is both small and large current with the same transducer. Finally, large temperature range, the low offset drift makes fluxgate technologies suitable for broad operation ranges. The technology has in general the limitations that is to require an external power source and an large noise level is observed when an AC component with frequency levels close to the even multiples of the sensor excitation frequency. This is superposed into the primary current. The research aims to discover a mean to reduce the disturbance effects on fluxgate sensors when an AC component is present in the primary current to be tested. It is found initially through measurements that there is high disturbances on the sensor output when the frequency of the AC component in the primary current coincides with the even multiples of the excitation frequency of the sensor. It is caused by an aliasing and the research presents one improvement to the problem in active compensation of AC components.

2 Basic structure of the fluxgate sensor

2.1 Structure

The fluxgate sensor [1] is used in the sensing of magnetic fields or electric currents, which operates on sudden drops in the non-linearity of the magnetic permeability of highly magnetic bodies near magnetic flux saturation. The structure of the fluxgate model used in the study is shown in Fig.1. It consists of a magnetic core in the form of a ring, a coil which supplies the drive voltage and picks up changes in current signal due to the primary current to be tested, *Ie* ,

which flows through the centre of the ring.

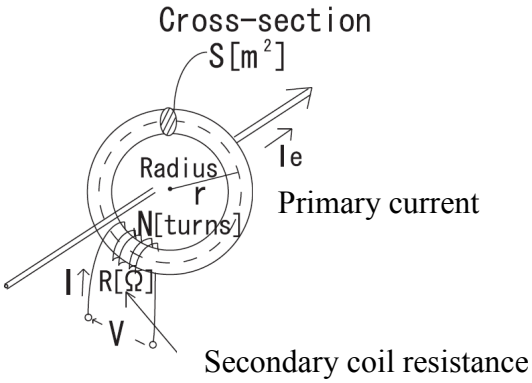

Figure 1: Diagram of a single core-type fluxgate direct current sensor

From the model of the fluxgate sensor in Fig.1, the following magnetic equations (2.1), (2.2), and (2.3) are obtained.

$$V(t) = RI(t) + N\frac{d\phi(t)}{\mathrm{dt}}$$

$$= RI(t) + NS\frac{dB(t)}{dt} \qquad (2.1)$$

$$2\pi rH(t) = NI(t) + I_e \qquad (2.2)$$

$$H(t) = (\frac{dH}{dB})(t) \cdot B(t) + H_0(t) \qquad (2.3)$$

And from the above equations, we have the block diagram as shown in Fig.2. A threshold current level is added to the step signal of the drive voltage so that it switches the sign when the magnetic core reaches saturation. The change in magnetic flux density is integrated in the dynamics of the sensor, and the signal is superposed with the primary current *Ie*, generates the internal current of the sensor, *I*.

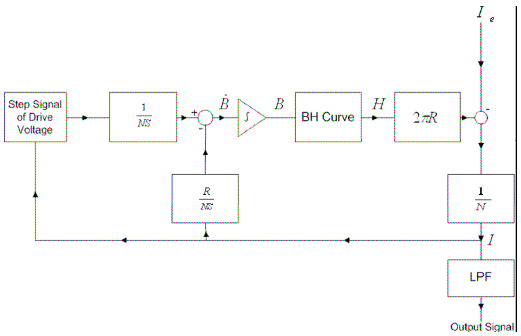

Figure 2: Block diagram of the fluxgate sensor operation

The drive voltage used in the model is a square wave, the corresponding output current in the presence of a DC input component. When *Ie*=0, the output current balances in the positive and negative region. When *Ie* >0, the magnetic flux generated by *Ie* is in the same direction as the flux generated by the output current, as a result of the overlapping in flux change, the positive pulse reaches saturation earlier than the negative pulse. By setting the drive voltage to switch when the magnetic core reaches saturation, a threshold current level, the difference in speed for the pulses to reach saturation is expressed by the time needed for the positive and negative such as Fig.3. This change is linearly proportional to the change in *Ie*.

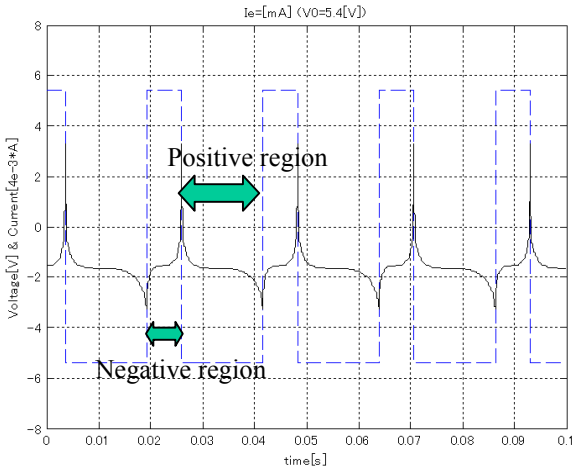

Figure 3: Voltage steps and current response in secondary winding (Primary current =2[A])

For the actual commercialized sensor, the internal current signal is converted to a voltage signal by passing it through a resistor and a low pass filter. The result is linearly related to *Ie*, thus the working of the fluxgate current sensor for DC analysis.

2.2 Aliasing

Aliasing [2] is a phenomenon which occurs when a sampling frequency is too low as compared to the original frequency of the analog signal. This results in a generation of a digital signal that has a spurious frequency that is different from the original frequency of the analog signal. In this event, there appears to be a high level of disturbance effect when the primary current, *Ie* has an AC component oscillating at frequency levels close to the even multiples of the excitation
frequency of the sensor. The occurrence of aliasing in the sensor was obtained through measurements, with the output signal being sinusoidal due to the AC component in the *Ie*, the peak-to-peak value is taken and the resulting frequency characteristics is shown in Fig.4. The sensor carries an excitation frequency of 56.5Hz and high disturbance effects in the output resulted when *Ie* contains an AC component that has a frequency close to the even multiples of the excitation frequency of the sensor. The peaks in Fig.4 coincides with the even multiples of the
excitation frequency of 56.5Hz.

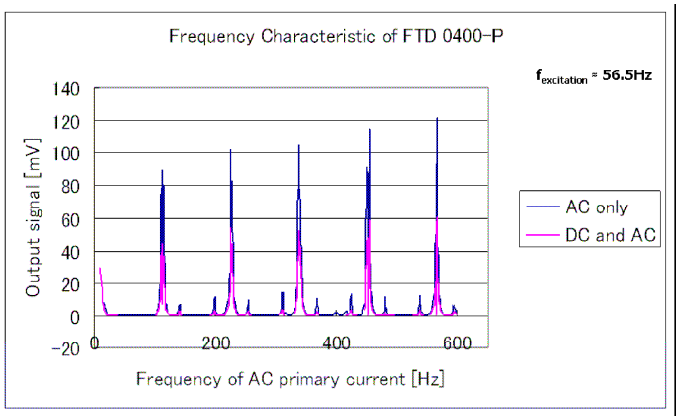

Figure 4: Frequency characteristics of FTD 0400-P

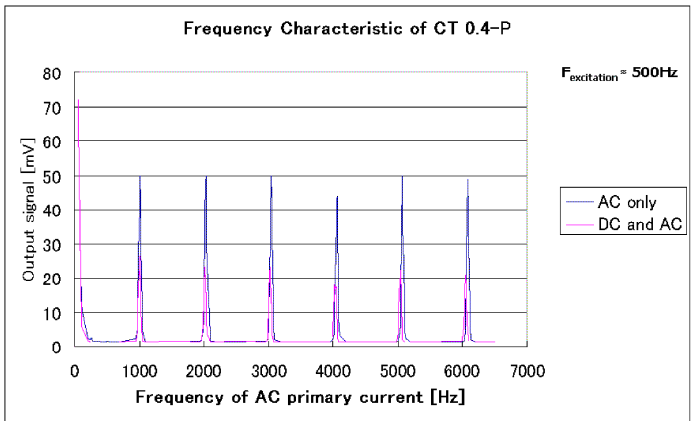

Figure 5: Frequency characteristics of Current Transducer 0.4-P

The phenomenon can be observed with another model of the fluxgate sensor that has an excitation frequency at 500Hz, Fig.5. The aliasing effect appears when the AC component in the input current has a frequency close to the even harmonic levels of the sensor.

2.2 The disturbance effects due to aliasing

There are several proposals for the elimination or the improvement on the effects from aliasing. Increase the sampling rate in the A/D conversion component of the sensor, anti-aliasing prefilter[3], multiple activation frequency model. However, these are inappropriate to increase in production cost and the lack in academic value. Active AC compensation method require an AC coil added to the existing sensor to pick up the primary current signals, DC component which is cancelled out through the use of a high pass filter or a band pass filter. The signal is then inverted and added back to the hysteresis comparator. Through accurate control in the amplitude gain and delay of the AC signal, it is possible to reduce the effect of aliasing in the sensor. This method is adopted in the study because it is capable for compensation for large disturbances.

2.3 Active AC compensation method

The adopted method for the cancellation of this disturbance effect due to aliasing is the active AC compensation method. In this method, an AC coil is added to the existing sensor to pick up the primary current signals. The DC component is cancelled out through the use of a band pass filter. The signal is inverted and returned to the hysteresis comparator as an inverted AC signal which cancels out the original AC component with accurate control in the gain and phase shift of the signal. A new block diagram is now shown in Fig.6.

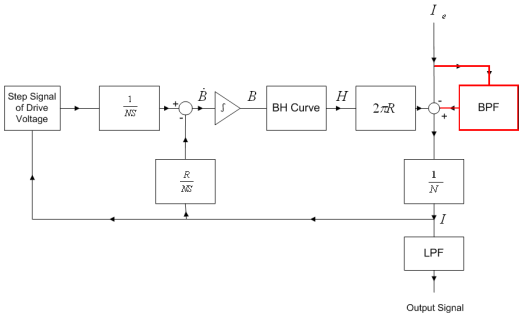

Figure 6: Block diagram with an Active AC-component compensation

The difference from the original system is the addition of a band pass filter to the original current input.

3 Simulation Results

Two simulation methods are used to assist the theoretical analysis, to check for the reliability and to help in the choosing of components for the actual measurements. The generic circuit simulator carries a circuit identical to the one used in the measurement. Another simulator, a dynamic response calculation using transition matrix of a linearized state space modeling is carried out in Matlab. This second simulator is less sophisticated and aims to check for the reliability of the generic circuit simulator.

3.1 Generic circuit generator

The simulation model with the generic circuit simulator may have shown a successful result in the aim to reduce the disturbance effects from AC components superposed into the external current input in a specific frequency level.

The bode diagram of the 2 band pass filters connected in series is shown in Fig.7.

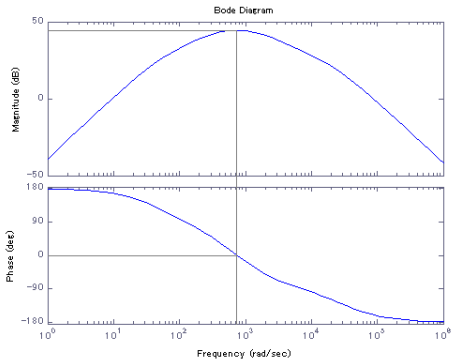

Figure 7: Bode diagram of functional block responsible for phase shift in AC signal

The bode diagram shows that the compensation signal is

inverted 180° at 700rad/sec which equates to 111Hz (1Hz = 2π rad/s). Since the excitation frequency of the sensor is at 60.5Hz, the sensor is tuned such that the aliasing effect is best cancelled out at the 2nd harmonic level. The excitation frequency of the sensor in this simulation is found to be at 60.5Hz. In the test for the AC compensation method in the simulation, the condition of AC component with amplitude of 1.0A at frequencies close to the even multiples of the excitation frequency is passed through the centre of the cores and the results between the condition of active compensation and the condition without compensation is observed. The complete data is shown in Table 1.

Table 1 Verification through simulation

f_{ac}=60.5Hz harmonic	Compensation Vpp(mV)	Output Vpp(mV)	Reduction %
2(120.0Hz)	69.3	175.8	60.5
4(241.6Hz)	95.7	186.0	48.5
6(362.8Hz)	119.7	164.7	27.3
8(483.7Hz)	116.8	145.7	19.9
10(604.8Hz)	95.9	128.2	25.0
12(725.8Hz)	94.8	116.5	18.6
14(846.8Hz)	85.2	107.6	20.9
20(1209.8Hz)	63.0	79.2	20.7

From the bode diagram drawn for the high pass filters the maximum compensation occurs at 111Hz. The highest reduction in the disturbance effect occurs at the 2*nd* harmonic level(120Hz). The effect of this active compensation is reduced as the frequency of the AC component rises, leading to the compensation signal being out of phase with the original signal, thus the cancellation effect works at best in a limited frequency region.

3.2 Dynamic response calculation using Matlab

A similar model is attempted using the state space modelling analysis with Matlab. The functions of the high pass filters as well as the low pass filter are added to the original program. The complete data is shown in Table 2

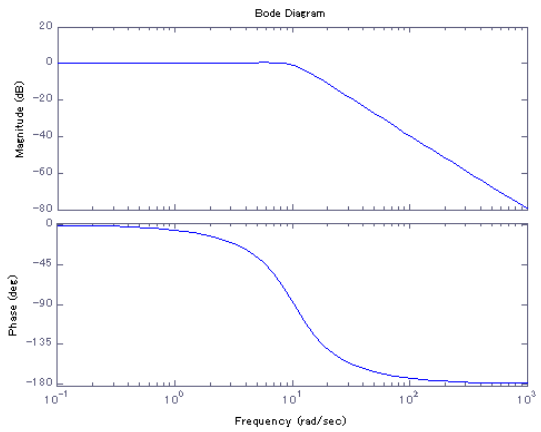

Figure 8: Bode diagram for LPF

Table 2 Verification through simulation

f_{ac}=58.1Hz harmonic	Compensation Vpp(mV)	Output Vpp(mV)	Reduction %
2(116Hz)	6.0	124.5	95.2
4(232Hz)	22.5	103.5	78.3
6(348Hz)	43.0	65.0	33.8
8(463Hz)	18.2	33.6	45.8
10(579Hz)	23.0	27.5	16.4
12(696Hz)	17.8	22.5	18.6

Compensation effect is observed through the transition matrix simulator. As predicted above, the highest level of compensation is observed at frequency range close to that of the 2*nd* harmonic level and gradually decreases as the compensation signal moves out of phase as the original current signal to be tested.

4 Experimental results

4.1 Effects of AC

In the simulation, the excitation frequency is at 60.5Hz whereas the experimental setup gives an excitation frequency of 54.0Hz. Next, alternating current with amplitude 1.0A is used as the primary current to be tested and the frequency is varied to observe the disturbance effects in the sensor output. The graphs for the output signals over the 2*nd* and 20*th* harmonic levels are shown from Fig.9 to Fig.12. The excitation frequency of the sensor is found to be at 54.0Hz and data for the 2*nd* and 20*th* harmonics are taken at 109.5Hz and 1079Hz, respectively. The AC component increases, the disturbance effects due to aliasing become smaller as shown in Fig.9 and Fig.12. Next it is found that at frequency levels exactly equal to the even multiples of the excitation frequency of the sensor, disturbance occurs but the signal is not a sinusoidal wave. As such, the emphasis in the study is focused onto the peak amplitude of the output signals rather than their frequency. The complete data is shown in Table 3.

Table 3 Verification through experiment

f_{ac}=54.0Hz harmonic	Compensation Vpp(mV)	Output Vpp(mV)	Reduction %
2(109.5Hz)	21.6	114.0	81.1
4(218.0Hz)	45.2	117.0	61.4
6(326.3Hz)	46.4	112.0	58.6
8(434.2Hz)	49.2	103.0	52.2
10(542.5Hz)	36.8	89.2	58.7
12(650.0Hz)	47.6	85.6	44.4
14(755.4Hz)	46.4	60.4	23.2
20(1079.0Hz)	40.8	46.4	12.1

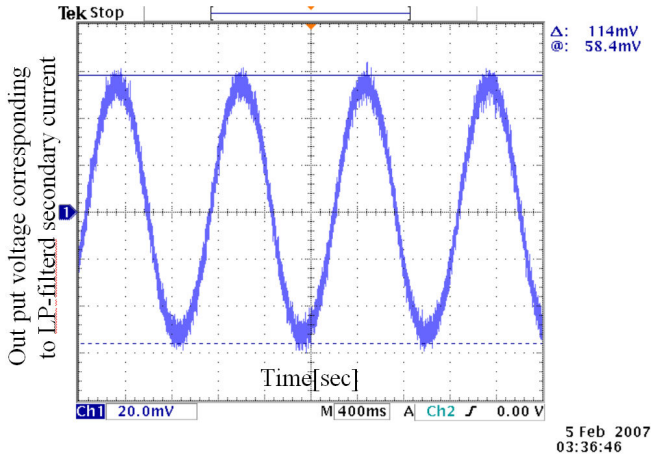

Figure 9: Normal output at 109.5Hz(2*nd* harmonic)

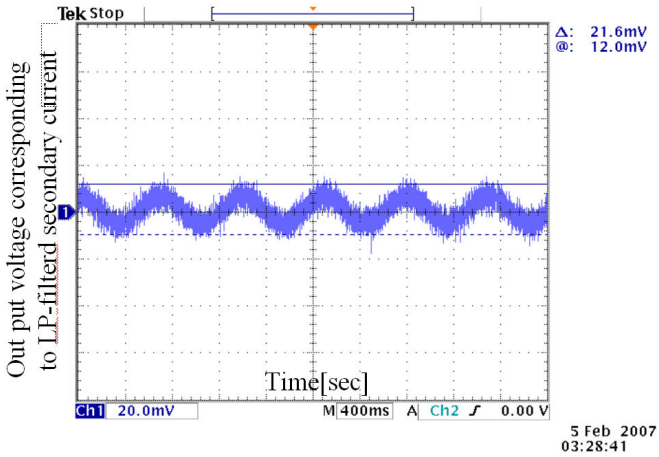

Figure 10: With compensation at 109.5Hz (2*nd* harmonic)

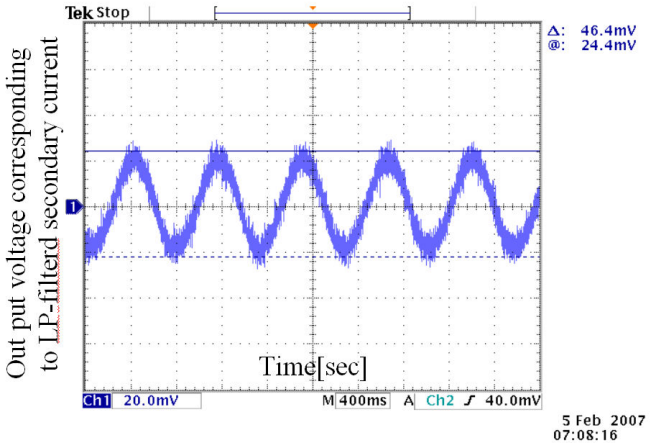

Figure 11: Normal output at 1079.0Hz (20*th* harmonic)

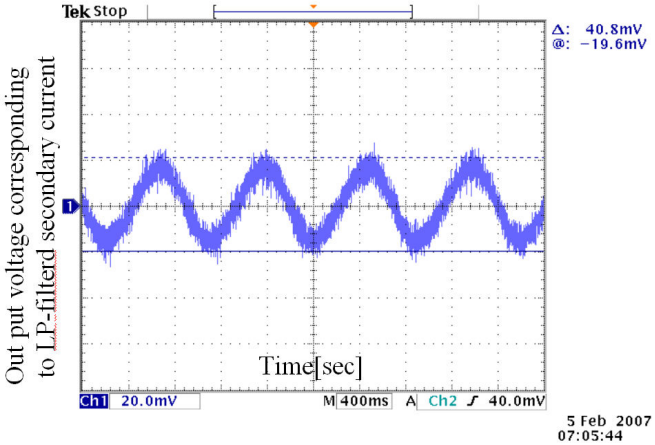

Figure 12: With compensation at 1079.0Hz (20*th* harmonic)

The difference in the level of disturbance reduction is due to the shift in the phase in the inverted AC compensation signal caused by the high pass filter. In comparison for the 2*nd* and 20*th* harmonic levels, the compensation signal is in phase while the other is considerably out of phase, thus, the difference in the percentage drop in the disturbance effects are shown in Table 2.

Also, for the phenomenon that the percentage-drop in disturbance appears more profound in experiments as compared to simulations. The reason is that in experiments, the frequency levels are adjusted analogically and the level for the highest disturbance effect is found easily whereas in the simulations, the frequency condition is given digitally and the sensitivity means that a shift by 0.1Hz brings a relatively high difference in the output levels.

4.5 Experimental evaluation of the AC compensation

The result of a reduction in the disturbance effects due to active AC compensation was seen in the measurements and with the high pass filters tuned to maximum compensation at the 2*nd* harmonic level. In conclusion, the AC compensation method in improving the disturbance effects due to aliasing is applicable.

5 Conclusion

For this compensation method with the aim to reduce the disturbance effects, the simulation and experiment results show that it is successful.

The maximum effect for this compensation can be tuned to a single frequency level but the compensation capability is less profound in other frequency levels due to inappropriate alteration of the phase of the compensated signal. In this research, the compensation was tuned to be at the maximum over the 2*nd* harmonic level because disturbance effects is the largest at the lower even harmonic regions.

REFERENCES

[1] Eiji Hashiguchi, ”Non-linear electromagnetic analysis of flux-gate coil system for designing sensitive current

sensors”, unpublished master’s thesis, the university of Tokyo *(in Japanese)* , 2006
[2] Jack Middlehurst, ”Practical Filter Design”Prentice Hall, 1993
[3] U.Tietze, ”Electronic Circuits Design and Applications” Springer-Verlag, 1991
[4] K.Mouri, ”Magbetic sensor science” Corona publishing, *(in Japanese)* 1998
[5] Y.Hori･K.Ounishi, ” Applied Control Engineering” Maruzen publishing, *(in Japanese)* 1998
[6] LEM, ” Isolated current and voltage transducers - Characteristics - Applications - Calculations”, 3rd Edition
[7] Y.Tanaki, “ Electric Circuit Simulator Pspice Entry-Level”, CQ publishiong, *(in Japanese)* 2003
[8]Y.Tanaki, “Electric Circuit Simulator Pspice Practice-Level”, CQ publishiong, *(in Japanese)* 2004